Synthesis of diblock copolymers with cellulose derivatives 4. Self-assembled nanoparticles of amphiphilic cellulose derivatives carrying a single pyrene group at the reducing-end

Yukiko Enomoto-Rogers, Hiroshi Kamitakahara*, Arata Yoshinaga, and Toshiyuki Takano

*Division of Forest and Biomaterials Science, Graduate School of Agriculture, Kyoto University, Kitashirakawa-Oiwake-cho, Sakyo-ku, Kyoto 606-8502, Japan; *Author for correspondence (e-mail: hkamitan@kais.kyoto-u.ac.jp; phone: +81-75-753-6255; fax: +81-75-753-6300)*

Abstract. Self-assembled cellulose-pyrene nanoparticles were prepared from amphiphilic cellulose derivatives carrying a single pyrene group at the reducing-end, *N*-(1-pyrenebutyloyl)-β-cellulosylamine (CELL13Py and CELL30Py, the number average degrees of polymerization (DP_n) of 13 and 30, respectively) and *N*-(15-(1-pyrenebutyloylamino)-pentadecanoyl)-β-cellulosylamine (CELL13C15Py and CELL30C15Py, DP_n of 13 and 30, respectively). Transmission electron microscopy (TEM) observation revealed that CELL13C15Py and CELL30C15Py formed self-assembled nanoparticles with the average diameters of 108.8 and 40.0 nm, respectively. The average radius of CELL30C15Py nanoparticles (20.0 nm) agreed well with the molecular length of its cellulose chain (19.2 nm). CELL30C15Py nanoparticles were expected to have monolayered structure, consisting of cellulose shell with radial orientation and hydrophobic core of 15-(1-pyrenebutyloylamino)-pentadecanoyl groups. The fluorescent spectrum of CELL30C15Py nanoparticles showed an excimer emission due to dimerized pyrene groups, indicating that the pyrene groups at the reducing-end of cellulose are associating in the particles. The balance of hydrophilic and hydrophobic parts of the cellulose derivatives controlled their self-assembled nanostructures. X-ray diffraction measurements revealed that radially oriented cellulose chains of CELL30C15Py nanoparticles were mostly amorphous, and at the same time exhibited weak reflection pattern of cellulose II, which is believed to have anti-parallel orientation.

Key Words cellulose; reducing-end; nanoparticle; self-assembly; radial orientation; fluorescent probe technique; pyrene.

Introduction

Cellulose is a linear (1→4)-β-glucopyranan having three hydroxyl groups at C2, C3, and C6 positions per anhydro glucose unit. The cellulose molecule has only one hemiacetal hydroxyl group at the reducing end, which can be substituted with other functional groups

with high regioselectivity. Focusing on the specific reactivity of the reducing-end group, we have succeeded to prepare cellulosic diblock copolymers by introducing long-chain alkyl groups into the reducing-end of cellulose chain (Kamitakahara et al. 2005; Kamitakahara and Nakatsubo 2005). Based on the same synthetic strategy, we have prepared copolymers with cellulose side-chains (Enomoto-Rogers et al. 2009a; Enomoto-Rogers et al. 2009b) and cellulose triacetate self-assembled gold nanoparticles (Enomoto-Rogers et al. 2010) to control self-assembly and orientation of cellulose chains. However, cellulose nanoparticles with radial orientation have not prepared yet, and their properties such as crystallinity are still unknown.

One of the most common nanoscaled cellulose material is cellulose nanocrystal, which can be prepared by acid hydrolysis (Habibi et al. 2010). The cellulose nanocrystal is usually needle-shaped bundle of cellulose chains, and its size is 5-20 nm wide and 100-2000 nm long. There have also been a few studies on sphere-shaped cellulose nanocrystal (Wang et al. 2008; Wang et al. 2007). The crystalline structure of these cellulose nanocrystals is the same as that of the original fibers, cellulose I in native form. Self-assembled cellulose nanoparticles organized in a radial manner with head-to-tail orientation have fundamentally different structure from cellulose nanocrystal prepared from native cellulose.

In general, cellulose I, the native form, is believed to have parallel orientation (Gardner and Blackwel.J 1974; Sugiyama et al. 1991). On the other hand, cellulose II, the regenerated or mercellized form, is believed to have anti-parallel orientation (Kolpak and Blackwell 1976; Langan et al. 1999). Cellulose crystals with parallel orientation have not yet been prepared in the solid state from regenerated cellulose or by chemical synthesis, although there have been some attempts using cello-oligosaccharide analogues (Bernet et al. 2000; Murty et al. 2006). Therefore, structure of cellulose chains organized in a radial manner with head-to-tail orientation is of considerable fundamental interest.

Recently, we have prepared amphiphilic cellulosic derivatives carrying a single pyrene group as a probe at the reducing-end. Fluorescent properties of pyrene revealed that these cellulose derivatives were self-assembled in NaOH aqueous solutions (Enomoto et al. 2006). The self-assembled cellulosic derivatives should have cellulose-shell and hydrophobic-core structure, where cellulose chains are oriented in a parallel or a radial manner. In the present report, we demonstrated the method to prepare self-assembled nanoparticles of amphiphilic cellulose derivatives carrying a long-chain alkyl group and a pyrene group. Effect of hydrophobic-hydrophilic balance of the compounds on their self-assembly systems and nanostructures were investigated by means of transmission electron microscopy (TEM) observations and fluorescent measurements.

Experimental

General Measurements

^{1}H-, ^{13}C-, and two-dimensional NMR spectra were recorded on a JEOL JNM-A500 FT-NMR (500 MHz) spectrometer, in $CDCl_3$ with tetramethylsilane (TMS) as an internal standard. Chemical shifts (δ) and coupling constants (J) are reported in (ppm) and (Hz), respectively. Fourier transform infrared (FT-IR) spectra were recorded on a Shimadzu FTIR-4000 spectrophotometer equipped with an ATR attachment (Durasampl IR-II).

GPC Measurement

Number and weight average molecular weights (M_n and M_w) and polydispersity index (M_w/M_n) were estimated by gel permeation chromatography (GPC) (SCL-10Avp, SIL-10A, LC-10Ai, CTO-10ACvp, RID-10A, Shimadzu, Japan) in chloroform at 40 ℃. Shodex columns (K-806M, K-802) were used. The flow rate was 0.8 ml/ min. Calibration curves were obtained by using polystyrene standards (Shodex).

TEM analysis

Transmission electron microscopy **(**TEM) images were collected by JEOL JEM-1220 system operating at an accelerating voltage of 100kV. The never-dried self-assembled cellulose-pyrene nanoparticles in methanol (ca. 0.1 mg/ ml) were dispersed again by stirring, and a portion of the obtained suspension was deposited on copper grids that were pre-coated by Formvar (polyvinyl formal) and reinforced by carbon, and stained with uranyl diacetate (UA). The sizes of particles were calibrated using Latex Particles ϕ0.23 μm (Ohken Shoji, Japan). TEM images were recorded on Fuji FG films (Fuji Film, Japan). TEM images were analyzed using public domain ImageJ program (Rasband, W.S., U. S. National Institutes of Health, Bethesda, Maryland, USA, http://rsb.info.nih.gov/ij/, 1997-2009).

Fluorescent measurements

Steady-state fluorescence spectra were recorded on a Shimadzu RF-5300PC spectrofluorophotometer. The never-dried self-assembled cellulose-pyrene nanoparticles in methanol (ca. 0.1 mg/ ml) were dispersed again by stirring, and a portion of the obtained suspension was loaded into a fluorescence cell, and analyzed in 1 min before precipitation occurred. All measurements were carried out at 25 ℃. They were recorded with an excitation wavelength of 350 nm. Excitation and emission slits were normally set at 5.0 nm. The excimer-to-monomer ratios (I_E/I_M) were calculated by taking the ratio of the emission intensity at ca. 470 nm to the half-sum of the emission intensities at 379 and 398 nm.

X-ray diffraction measurements

X-ray diffraction measurements were carried out with a Rigaku diffractometer Ultima IV. A Nickel-filtered CuKα radiation was used at 40 kV and 30 mA. Cellulose microcrystalline (Avicel, Merck) and low-molecular-weight cellulose was used to obtain reflection pattern of cellulose I and cellulose II, respectively.

Materials

N-(1-Pyrenebutyloyl)-tri-*O*-acetyl-β-cellulosylamine, CTA13Py (DP_n=13) and CTA30Py (DP_n=30), and *N*-(15-(1-pyrenebutyloylamino)-pentadecanoyl)-tri-*O*-acetyl-β-cellulosylamine CTA13C15Py (DP_n=13) and CTA30C15Py (DP_n=30), cellulose triacetates (CTA13 (DP_n=13) and CTA30 (DP_n=30)) were prepared as described in the previous article (Enomoto et al. 2006; Kamitakahara et al. 2005). Number and weight average molecular weights (M_n and M_w) and polydispersity index (M_w/M_n) of acetylated cellulose derivatives were estimated by GPC measurements using polystyrene standards. Number average degrees of polymerization (DP_n) of cellulose chains of the derivatives were calculated from peak ratio of pyrene groups to ring protons in the ^{1}H-NMR spectra. The theoretical molecular lengths of cellulose derivatives were calculated from degrees of polymerization determined by NMR analysis. Low-molecular-weight cellulose (DP_n=13) was prepared from cellulose microcrystalline (CF-11, Whatman) using phosphoric acid according to previous article (Atalla et al. 1984; Isogai and Usuda 1991). Cellulose microcrystalline (Avicel, Merck), cellulose microcrystalline (CF-11, Whatman), 1,8-diazabicyclo[5,4,0]-7-undecene (DBU) and all other reagents were commercially obtained and used without further purification.

N-(1-pyrenebutyloyl)-β-cellulosylamine (CELL13Py and CELL30Py)

To a solution of *N*-(1-pyrenebutyloyl)-tri-*O*-acetyl-β-cellulosylamine, CTA13Py (DP_n=13) (3.0 mg) in methanol/ 1,4-dioxane (1:4, 0.3 ml), DBU (30 μl, 0.02 mmol) was added at room temperature, and stirred for 4 h under the nitrogen. The precipitated compounds were washed with methanol to remove DBU, and then methanol and DBU were removed by decantation to avoid collapse of the particles. This procedure was repeated at least five times. The precipitated compounds were preserved in methanol. For sample preparation, the precipitated compounds in methanol were dispersed again by stirring, and a portion of the obtained suspension was loaded into a cell for fluorescent measurements or deposited on a copper grid for TEM observations. For X-ray analysis, methanol in the suspension of nanoparticles were replaced with water by decantation, and freeze-dried to obtain the powder of cellulose nanoparticles of *N*-(1-pyrenebutyloyl)-β-cellulosylamine, CELL13Py (DP_n=13) (1.3 mg, 81.2%). The complete deacetylation of the cellulose derivatives was confirmed by FT-IR spectrum with disappearance of absorbance of acetyl group at 1755 cm^{-1} (C=O) and

appearance of absorbance of hydroxyl group at 3400 cm^{-1} (OH). The same procedure was applied to CTA30Py (DP_n=30) (3.0 mg), to give *N*-(1-pyrenebutyloyl)-β-cellulosylamine CELL30Py (DP_n=30) (1.0 mg, 66.7%).

N-(15-(1-pyrenebutyloylamino)-pentadecanoyl)-β-cellulosylamine (CELL13C15Py and CELL30C15Py)

The deprotection and self-assembly procedures described above were applied to *N*-(15-(1-pyrenebutyloylamino)-pentadecanoyl)-tri-*O*-acetyl-β-cellulosylamine, CTA13C15Py (DP_n=13) (10.3 mg) and CTA30C15Py (DP_n=30) (9.0 mg), to give cellulose nanoparticles of *N*-(15-(1-pyrene-butyloylamino)-pentadecanoyl)-β-cellulosylamine, CELL13C15Py (DP_n=13) (2.8 mg, 50.0%) and CELL30C15Py (DP_n=30) (2.7 mg, 54.0%), respectively.

Regenerated cellulose (CELL13 and CELL30)

CTA13 (DP_n=13) (30.0 mg) and CTA30 (DP_n=30) (30.0 mg) were deacetylated in the same manner described above to give regenerated cellulose, CELL13 (DP_n=13) (9.8 mg, 58.3%) and CELL30 (DP_n=30) (10.4 mg, 61.9%), respectively.

Results and Discussion

Preparation of amphiphilic cellulose nanoparticles

Pyrene exhibits the monomer emission (intensity I_M, ca. 380 nm) when it is isolated from each other. Two pyrene molecules form excited dimer (excimer), and exhibit a broad structureless excimer emission (intensity I_E, ca. 480 nm) when they are associated in symmetrical sandwich arrangement at a distance of ca. 3.5 Å (Birks 1970). The formation of pyrene aggregate or hydrophobic domain can be confirmed by the presence of the pyrene excimer emission, and the ratio I_E/I_M can be used to evaluate the association system of pyrenes (Winnik et al. 1987). Diffusion and association of hydrophobic groups at the reducing-end of cellulose can be confirmed by the monomer and excimer emission of pyrenes, respectively, when a single pyrene group is regioselectively introduced to the reducing-end of the cellulose backbone.

Regarding a method to prepare self-assembled nanoparticles, nanoprecipitation is known as an effective way to prepare nanoparticles of amphiphilic polymers including cellulose esters or dextran esters out of organic/water solvent mixture, for example by dialysis or oil/water emultion method. (Hornig and Heinze 2008; Hornig et al. 2005; Kataoka et al. 2001; Lassalle and Ferreira 2007; O'Reilly et al. 2006). Amphiphilic cellulosic derivatives

carrying a long-chain alkyl and pyrene groups were not soluble in common organic solvents, such as chloroform or *N*,*N*-dimethyl formamide, as reported in our previous article (Enomoto et al. 2006). We anticipated that nanoparticles of amphiphilic cellulosic derivatives could be prepared *via* deprotection of acetylated cellulose derivatives in an organic solvent and self-assembly of the resulting amphiphilic cellulose derivatives in a nonsolvent, such as methanol.

N-(1-Pyrenebutyloyl)-β-cellulosylamine (CELL13Py (DP_n=13) and CELL30Py (DP_n=30)) and *N*-(15-(1-pyrenebutyloylamino)-pentadecanoyl)-β-cellulosylamine (CELL13C15Py (DP_n=13) and CELL30C15Py (DP_n=30)) were prepared through the deprotection of corresponding acetylated derivatives with an alkaline reagent, DBU in methanol/ 1,4-dioxane (1:4) mixed solvent. Regenerated cellulose without hydrophobic groups, CELL13 and CELL30 were prepared from cellulose triacetate (DP_n=13 and 30, respectively) in the same procedure as control experiments. The chemical structures of the cellulose derivatives are shown in Figure 1. Characteristics of these cellulose derivatives are summarized in Table 1. The theoretical molecular lengths of cellulose derivatives were calculated from degrees of polymerization determined by NMR analysis of corresponding acetylated cellulose derivatives. The amide linkages between C1 and pentadecanoyl group (-C1-NH-CO-) and between pentadecanoyl group and pyrenebutyloyl group (-CH_2-NH-CO-$(CH_2)_3$-Py) are stable under the alkaline condition using DBU (Enomoto et al. 2006). The cellulose derivatives did not precipitate in the solvent system during the reaction, likely due to the ionization of hydroxyl groups of cellulose. Preparation of nanoparticles was carried out by a combination of deprotection and self-assembly of the cellulose derivatives. The reaction mixture of the cellulose derivatives in methanol/ 1,4-dioxane was added dropwise into a larger amount of methanol, which is a poor solvent for cellulose, and allowed to stand overnight. The deprotected cellulose derivatives precipitated as nanoparticles, as discussed in the next sections, through a quite slow self-assembly in methanol. When the deprotection was carried out using sodium methoxide as an alkaline reagent in methanol/ chloroform, the deprotected derivatives precipitated as disordered and irregular aggregates in few hours. The precipitates of deprotected cellulose derivatives were washed with methanol, and methanol and DBU were removed by decantation. Those precipitates were insoluble and not dispersed as colloids in water or other common organic solvents such as *N*,*N*-dimethyl formamide or dimethyl sulfoxide, and never formed suspension again in methanol or water when they were dried. The samples for TEM analysis and fluorescent measurements were prepared from the suspension of never-dried cellulose derivatives.

Nanostructures of self-assembled cellulose-pyrene nanoparticles

Nanostructures of the cellulose derivatives were analyzed by TEM. The TEM images of cellulose and cellulose derivatives are shown in Figure 2. CELL13, CELL13Py, CELL30,

and CELL30Py formed irregular aggregates, which were positively stained with UA, as shown in Figures 2a, 2b, 2e, and 2d, respectively. However, in the case of cellulose derivatives carrying long-chain alkyl and pyrene groups, CELL13C15Py and CELL30C15Py, the nanoparticles were observed as shown in Figures 2c and 2f. These nanoparticles were negatively stained with UA, suggesting crystallization or stronger packing of cellulose chains, compared to other irregular aggregates of cellulose. The size distribution histograms, average diameter (AVE), and standard deviation (SD) of CELL13C15Py and CELL30C15Py obtained by TEM analysis are shown in Figure 3. The CELL13C15Py and CELL30C15Py nanoparticles tended not to disperse individually on a copper grid due to a strong interaction between particles, resulting in the production of large interparticle aggregates. Consequently, we found the well-dispersed particles as shown in Figures 2c and 2f. The well-dispersed particles exist in the top half of Figure 2f, and the interparticle aggregates exist in the bottom half and the black-colored bottom end of Figure 2f. Due to low contrast of the aggregates, we could not identify sufficient number of the particles to measure their size, and, as a result, could not calculate their deviation. However, we confirmed the reproducibility of data obtained by fluorescent and XRD measurements. This fact also supports the reproducibility of the structure of the cellulosic nanoparticles. The same phenomena such as interparticle aggregation is reported in previous articles on spherical cellulose nanocrystals prepared by hydrolysis of cellulose microcrystals (Wang et al. 2008; Wang et al. 2007). The suspension of the cellulose nanoparticles obtained in this study was stable in methanol after a couple of months.

The average diameter of CELL13C15Py nanoparticles was 108.8 nm. The edge of particles was clearly stained, suggesting a strong packing of cellulose chains or stability of the nanoparticles. It was suggested that CELL13C15Py formed self-assembled nanoparticles due to hydrophobic interactions between 15-(1-pyrenebutyloylamino)-pentadecanoyl groups. No hollow was observed in TEM images of CELL13C15Py nanoparticles. In addition, the theoretical molecular length of CELL13C15Py is 9.4 nm, and this value is rather smaller than the radius of CELL13C15Py nanoparticles (54.4 nm) as shown in Figure 2c. Consequently, it was suggested that CELL13C15Py nanoparticles were not monolayered. It was, however, difficult to investigate further detailed structures inside the nanoparticle.

CELL30C15Py formed smaller nanoparticles with the average diameter of 40.0 nm compared to CELL13C15Py nanoparticles, and the standard deviation of their diameters was smaller than that of CELL13C15Py. The enlarged image of Figure 2f is shown in Figure 4a. The theoretical molecular length of CELL30C15Py was calculated to be 19.2 nm. The radius of CELL30C15Py nanoparticles (20.0 nm) agreed well with its molecular length. It was suggested that CELL30C15Py nanoparticles were monolayered, consisting of cellulose shell with radial orientation and hydrophobic core of long-chain alkyl group. Pyrene group should be located inside of the hydrophobic domain. The structural image of a single cellulose nanoparticle of CELL30C15Py was illustrated in Figure 4b. The deviations of

diameter of nanoparticles are likely due to the polydispersity of cellulose chains. Consequently, the novel self-assembled nanoparticles of amphiphilic cellulose derivatives were successfully prepared through the deprotection of acetyl groups under alkaline condition and the subsequent slow self-assembly. A hydrophilic-hydrophobic balance in one molecule controlled their self-assembled nanostructures.

Fluorescent studies of self-assembled cellulose-pyrene nanoparticles

The association system of self-assembled cellulose-pyrene nanoparticles was investigated by means of the fluorescent probe method. Fluorescence spectra of the suspension of the never-dried self-assembled cellulose-pyrene nanoparticles in methanol were measured after the nanoprecipitation and removal of DBU. The fluorescence spectra of the cellulose derivatives are shown in Figure 5. The CELL13Py and CELL30Py showed the strong monomer emission (at ca. 380 and 390 nm) due to a locally excited pyrene, as shown in Figures 5a and 5c. The I_E/I_M values of CELL13Py (I_E/I_M = 0.18) and CELL30Py (I_E/I_M = 0.11) remained low, indicating that the pyrenes of these derivatives diffused and did not associate.

On the other hand, CELL13C15Py and CELL30C15Py having a long-chain alkyl group, exhibited the excimer emission due to pyrene dimer (at ca. 470 nm) besides the monomer emission, as shown in Figures 5b and 5d. The I_E/I_M values of CELL13C15Py (I_E/I_M = 0.41) and CELL30C15Py (I_E/I_M = 0.23) took higher values, compared to CELL13Py (I_E/I_M = 0.18) and CELL30Py (I_E/I_M = 0.11). The spectra imply that hydrophobic alkyl and pyrene groups at the reducing-end of CELL13C15Py and CELL30C15Py associated in the nanoparticles. The excimer emission of CELL13C15Py and CELL30C15Py are assigned to stronger hydrophobic interactions of pyrene groups anchored at the end of long-chain alkyl group, compared to CELL13Py or CELL30Py. The CELL13C15Py, with higher composition of hydrophobic groups in the molecule, took higher I_E/I_M value, and formed larger nanoparticles than those in CELL30C15Py as shown in TEM images in Figure 2c. Namely, more pyrene groups associated in the nanoparticles of CELL13C15Py with relatively stronger hydrophobic interactions, compared to those in CELL30C15Py nanoparticles.

Excimer emission of pyrenes originates from a “dynamic” pyrene dimer due to two pyrene molecules which are in collision with each other when excited, or a “static” pyrene dimer due to the pyrenes associated prior to excitation (Birks 1970). In general, for dynamic excimers, excitation spectra for the monomer (monitored at ca. 380 nm) and the excimer (monitored at ca. 470 nm) show the same peak patterns and positions. However, for “static” preassociated pyrene excimers which is formed before excitation, the spectrum for the excimer emission shows red-shift (ca. 1 to 8 nm) compared with that for the monomer emission, although they are identical in band patterns (Winnik 1990; Winnik et al. 1987; Winnik et al. 1998). The excitation spectra of CELL13C15Py and CELL30C15Py were measured to distinguish the

origin of the excimer emission, and are shown in Figure 6. The spectrum for the excimer monitored at 470 nm showed red-shift of ca. 2-5 nm, compared to that for the monomer monitored at 380 nm. Those facts indicated that the excimer emission of CELL13C15Py and CELL30C15Py originated from the "static" pyrene dimers (preassociated aggregates), not from the "dynamic" pyrene dimers. Those spectra, in the cases of CELL13C15Py and CELL30C15Py, support that those amphiphilic cellulose derivatives self-assembled to form nanoparticles promoted by the hydrophobic interaction between 15-(1-pyrenebutyloylamino)-pentadecanoyl groups.

X-ray diffraction measurements

In general, cellulose I, the native form, is believed to have parallel orientation. (Gardner and Blackwel.J 1974; Sugiyama et al. 1991). On the other hand, cellulose II, the regenerated or mercellized form, is believed to have anti-parallel orientation (Kolpak and Blackwell 1976; Langan et al. 1999). X-ray diffraction measurements were carried out to analyze crystalline pattern of self-assembled cellulose-pyrene nanoparticles. The diffraction angle and *d* spacings of cellulose and self-assembled cellulose-pyrene nanoparticles are summarized in Table 2. Cellulose chains of all derivatives had quite low crystallinity as shown in Figures 7. CELL30 and CELL30Py showed no crystalline pattern as shown in Figures 7d and 7e. In the case of CELL13 (Figure 7a), CELL13Py (Figure 7b), and CELL13C15Py (Figure 7c), the observed weak diffraction patterns were those of typical cellulose II (Figure 7h), with three strong $(1\bar{1}0)$, (110), and (200) reflections located at d = 0.739, 0.451, and 0.407 nm, respectively (Isogai et al. 1989). Regarding the fact that CELL13, CELL13Py, and CELL13C15Py did not show monolayered structure in TEM images, their cellulose chains may have anti-parallel orientation. On the other hand, CELL30C15Py nanoparticles consisting of radially oriented cellulose also exhibited crystalline pattern of cellulose II (Figure 7f). In other words, it is likely that not only anti-parallel but also radial and head-to-tail orientations of cellulose chains give a crystal structure of cellulose II.

Conclusions

Self-assembled cellulose-pyrene nanoparticles of CELL13C15Py and CELL30C15Py were successfully prepared by deprotection in methanol/ 1,4-dioxane using DBU and the self-assembly in methanol. The novel method to control the supramolecular structures of diblock-type amphiphilic cellulose derivatives was demonstrated. The hydrophilic-hydrophobic balance of the molecule controlled the size and structures of the nanoparticles. In particular, the average radius of CELL30C15Py nanoparticles agreed well with its molecular length. The CELL30C15Py nanoparticles should have monolayered

structure with radially oriented cellulose chains. The CELL30C15Py nanoparticles exhibited weak reflection pattern of cellulose II.

Acknowledgement

We acknowledge Graduate School of Agricultural and Life Sciences, the University of Tokyo, for 500-MHz NMR and GPC equipments. This study was supported in part by a Grand-in-Aid from a Research Fellowships of the Japan Society for the Promotion of Science (JSPS) for Young Scientists (Y.E-R), and by a Grant-in-Aid for Scientific Research from the Ministry of Education, Science, and Culture of Japan (Nos. 18688009 and 21580205).

References

Atalla, R.H., Ellia, J.D. and Schroeder, L.R. (1984) Some effects of elevated temperatures on the structure of cellulose and its transformation. Jounal of Wood Chemistry and Technology 4:465-482.

Bernet, B., Xu, J.W. and Vasella, A. (2000) Oligosaccharide analogues of polysaccharides part 20 - NMR analysis of templated cellodextrins possessing two parallel chains: A mimic for cellulose I? Helvetica Chimica Acta 83:2072-2114.

Birks, J.B., (1970) Photophysics of aromatic molecules. Wiley-Interscience, London, p. 1.

Enomoto-Rogers, Y., Kamitakahara, H., Nakayama, K., Takano, T. and Nakatsubo, F. (2009a) Synthesis and thermal properties of poly(methyl methacrylate)-graft-(cellobiosylamine-C15). Cellulose 16:519-530.

Enomoto-Rogers, Y., Kamitakahara, H., Takano, T. and Nakatsubo, F. (2009b) Cellulosic graft copolymer: poly(methyl methacrylate) with cellulose side chains. Biomacromolecules 10:2110-2117.

Enomoto-Rogers, Y., Kamitakahara, H., Yoshinaga, A. and Takano, T. (2010) Radially oriented cellulose triacetate chains on gold nanoparticles. Cellulose 17:923-936.

Enomoto, Y., Kamitakahara, H., Takano, T. and Nakatsubo, F. (2006) Synthesis of diblock copolymers with cellulose derivatives. 3. Cellulose derivatives carrying a single pyrene group at the reducing-end and fluorescent studies of their self-assembly systems in aqueous NaOH solutions. Cellulose 13:437-448.

Gardner, K.H. and Blackwel.J (1974) Structure of Native Cellulose. Biopolymers 13:1975-2001.

Habibi, Y., Lucia, L.A. and Rojas, O.J. (2010) Cellulose nanocrystals: Chemistry, self-assembly, and applications. Chemical Reviews 110:3479-3500.

Hornig, S. and Heinze, T. (2008) Efficient approach to design, stable water-dispersible nanoparticles of hydrophobic cellulose esters. Biomacromolecules 9:1487-1492.

Hornig, S., Heinze, T., Hesse, S. and Liebert, T. (2005) Novel nanoparticles based on dextran esters with unsaturated moieties. Macromolecular Rapid Communications 26:1908-1912.

Isogai, A. and Usuda, M. (1991) Preparation of low-molecular-weight celluloses using phosphoric-acid. Mokuzai Gakkaishi 37:339-344.

Isogai, A., Usuda, M., Kato, T., Uryu, T. and Atalla, R.H. (1989) Solid-state CP MAS C13 NMR-study of cellulose polymorphs. Macromolecules 22:3168-3172.

Kamitakahara, H., Enomoto, Y., Hasegawa, C. and Nakatsubo, F. (2005) Synthesis of diblock copolymers with cellulose derivatives. 2. Characterization and thermal properties of cellulose

triacetate-block-oligoamide-15. Cellulose 12:527-541.

Kamitakahara, H. and Nakatsubo, F. (2005) Synthesis of diblock copolymers with cellulose derivatives. 1. Model study with azidoalkyl carboxylic acid and cellobiosylamine derivative. Cellulose 12:209-219.

Kataoka, K., Harada, A. and Nagasaki, Y. (2001) Block copolymer micelles for drug delivery: design, characterization and biological significance. Advanced Drug Delivery Reviews 47:113-131.

Kolpak, F.J. and Blackwell, J. (1976) Determination of structure of cellulose II. Macromolecules 9:273-278.

Langan, P., Nishiyama, Y. and Chanzy, H. (1999) A revised structure and hydrogen-bonding system in cellulose II from a neutron fiber diffraction analysis. Journal of the American Chemical Society 121:9940-9946.

Lassalle, V. and Ferreira, M.L. (2007) PLA nano- and microparticles for drug delivery: An overview of the methods of preparation. Macromolecular Bioscience 7:767-783.

Murty, K.V.S.N., Xie, T., Bernet, B. and Vasella, A. (2006) Oligosaccharide analogues of polysaccharides - Part 26 - Mimics of cellulose I and cellulose II: Di- and monoalkynyl C-cellosides of 1,8-disubstituted anthraquinones. Helvetica Chimica Acta 89:675-730.

O'Reilly, R.K., Hawker, C.J. and Wooley, K.L. (2006) Cross-linked block copolymer micelles: Functional nanostructures of great potential and versatility. Chemical Society Reviews 35:1068-1083.

Sugiyama, J., Vuong, R. and Chanzy, H. (1991) Electron-diffraction study on the 2 crystalline phases occurring in native cellulose from an algal cell-wall. Macromolecules 24:4168-4175.

Wang, N., Ding, E. and Cheng, R.S. (2008) Preparation and 'liquid crystalline properties of spherical cellulose nanocrystals. Langmuir 24:5-8.

Wang, N., Ding, E.Y. and Cheng, R.S. (2007) Thermal degradation behaviors of spherical cellulose nanocrystals with sulfate groups. Polymer 48:3486-3493.

Winnik, F. (1990) Fluorescence studies of aqueous-solutions of poly(N-isopropylacrylamide) below and above their LCST. Macromolecules 23:233-242.

Winnik, F., Winnik, M., Tazuke, S. and Ober, C. (1987) Synthesis and characterization of pyrene-labeled (hydroxypropyl)cellulose and its fluorescence in solution. Macromolecules 20:38-44.

Winnik, M., Bystryak, S., Liu, Z. and Siddiqui, J. (1998) Synthesis and characterization of pyrene-labeled poly(ethylenimine). Macromolecules 31:6855-6864.

Figure Legend

Figure 1. Chemical structures of cellulose derivatives, CELL13Py, CELL13C15Py, CELL30Py, and CELL30C15Py.

Figure 2. TEM images of (a) CELL13, (b) CELL13Py, (c) CELL13C15Py, (d) CELL30, (e) CELL30Py, and (f) CELL30C15Py dispersed in methanol.

Figure 3. Size distributions of the diameters of (a) CELL13C15Py and (b) CELL30C15Py, analyzed by TEM observation.

Figure 4. (a) Enlarged TEM image of Figure 2f and (b) structural image of CELL30C15Py nanoparticle.

Figure 5. Fluorescence spectra of pyrene of (a) CELL13Py, (b) CELL13C15Py, (c) CELL30Py, and (d) CELL30C15Py. 0.1 mg/ ml in methanol. λ_{ex} = 350 nm, 25℃.

Figure 6. Excitation spectra of (a) CELL13C15Py and (b) CELL30C15Py in methanol monitored at 380 nm (monomer) (solid line) and at 470 nm (excimer) (dashed line).

Figure 7. Wide angle X-ray diffractgrams of (a) CELL13, (b) CELL13Py, (c) CELL13C15Py, (d) CELL30, (e) CELL30Py, (f) CELL30C15Py, (g) microcrystalline cellulose (cellulose I), and (h) regenerated cellulose (cellulose II).

Table 1. Characteristics of regenerated cellulose and cellulose derivatives.

Table 2. Diffraction angle and *d* spacings of cellulose and self-assembled cellulose-pyrene nanoparticles.

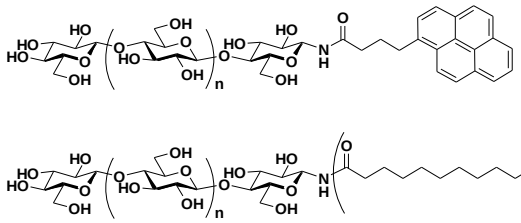

Cell13Py : n=11
Cell30Py : n=28

Cell13C15Py : n=11, m=1
Cell30C15Py : n=28, m=1

Figure 1 Chemical Structures of cellulose derivatives, **Cell13Py**, **Cell13C15Py**, **Cell30Py**, **Cell30C15Py**.

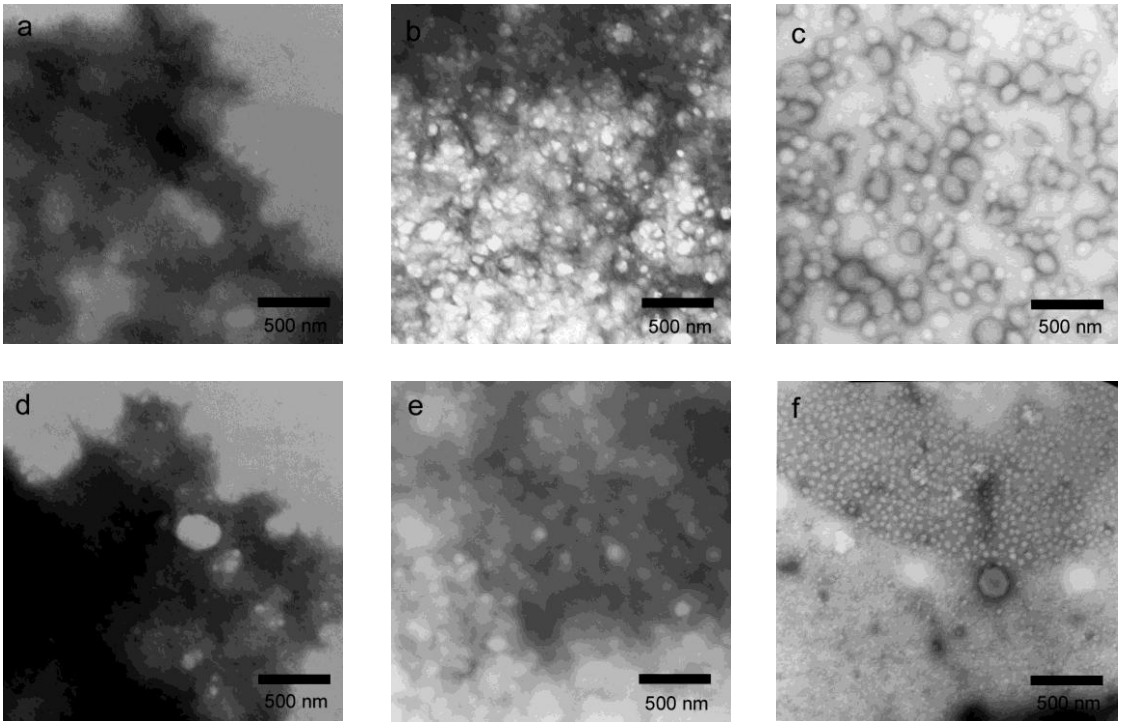

Figure 2. TEM images of (a) CELL13, (b) CELL13Py, (c) CELL13C15Py, (d) CELL30, (e) CELL30Py, and (f) CELL30C15Py dispersed in methanol.

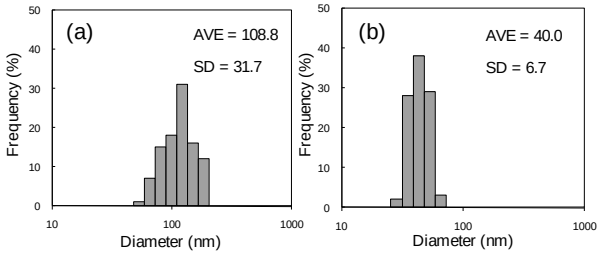

Figure 3. Size distributions of the diameters of (a) CELL13C15Py and (b) CELL30C15Py, analyzed by TEM observation.

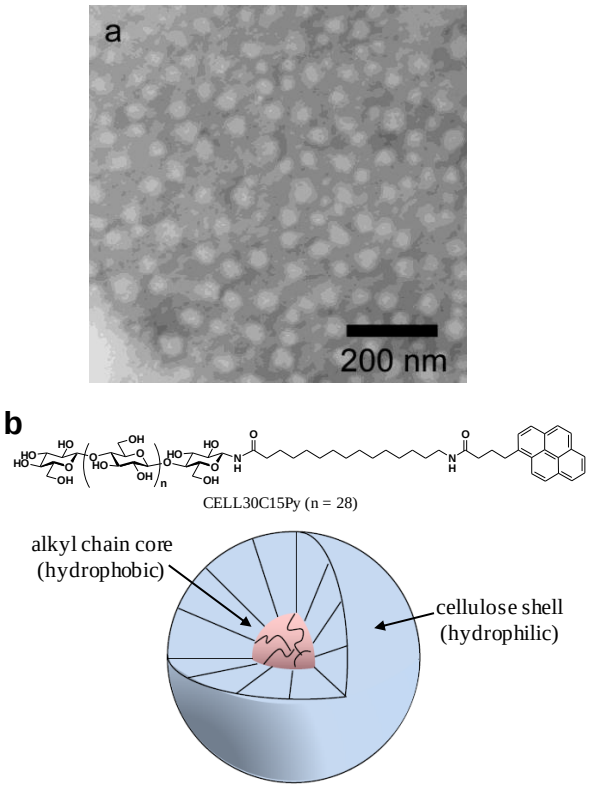

Figure 4. (a) Enlarged TEM image of Figure 2f and (b) structural image of CELL30C15Py nanoparticle.

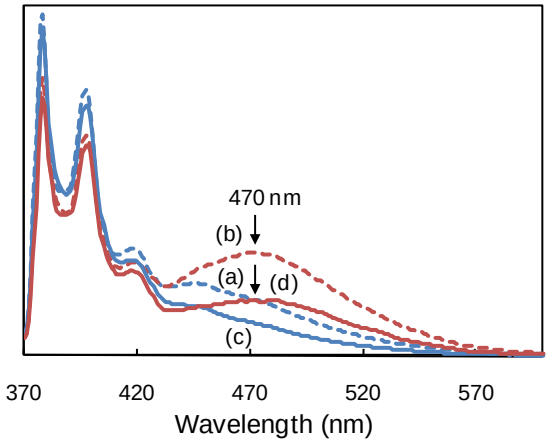

Figure 5 Fluorescence spectra of pyrene of (a) CELL13Py, (b) CELL13C15Py, (c) CELL30Py, and (d) CELL30C15Py. 0.1 mg/ml in methanol. λ_{ex} = 350 nm, 25℃.

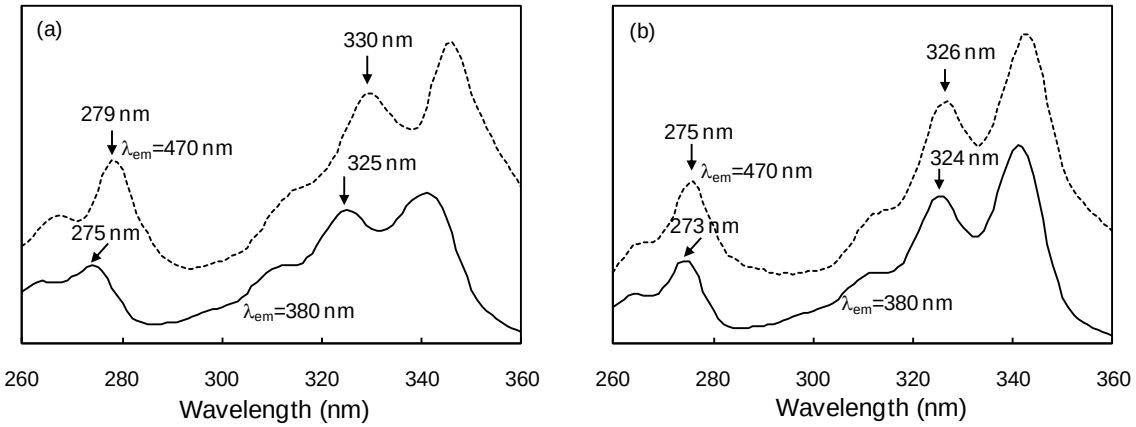

Figure 6. Excitation spectra of (a) CELL13C15Py and (b) CELL30C15Py in methanol monitored at 380 nm (monomer) (solid line) and at 470 nm (excimer) (dashed line).

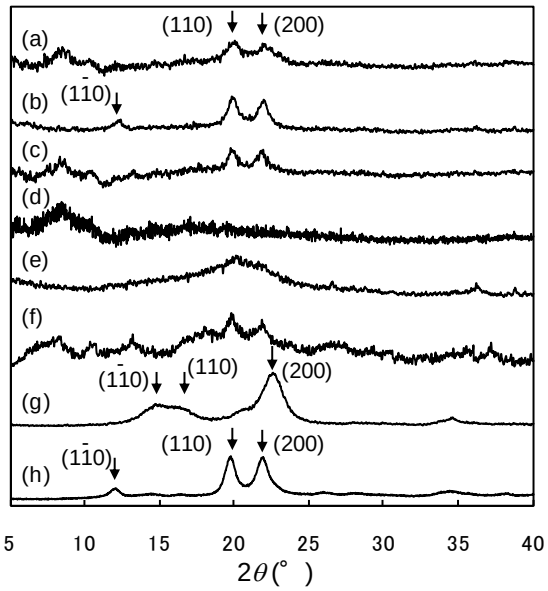

Figure 7. Wide angle X-ray diffractgrams of (a) CELL13, (b) CELL13Py, (c) CELL13C15Py, (d) CELL30, (e) CELL30Py, (f) CELL30C15Py, (g) microcrystalline cellulose (cellulose I), and (h) regenerated cellulose (cellulose II).

Table 1. Characteritics of regenerated cellulose and cellulose derivatives.

Cellulose derivatives	M_n (10^{-4})[a]	PDI [a]	DP_n of cellulose chain calculated from M_n[a]	DP_n of cellulose chain calculated by NMR analysis[b]	Theoretical molecular length of cellulose chain (nm)[c]	Theoretical molecular length of one molecule (nm)[e]
CELL13	0.37	1.30	13	-	6.4[d]	6.4
CELL13Py	0.47	1.40	15	11	5.5	6.7
CELL13C15Py	0.48	1.50	15	12	6.0	9.4
CELL30	0.85	1.83	30	-	15.0[d]	15.0
CELL30Py	1.18	1.81	40	27	13.5	14.7
CELL30C15Py	1.28	1.75	43	32	15.8	19.2

[a] Number average molecular weight and polydispersity index (PDI) of acetylated derivatives calculated by GPC analysis using PS standards. [b] Calculated from integral areas of ring protons and pyrene aromatic protons of the acetylated derivatives. [c] Calculated from DP_n determined by NMR analysis. [d] Calculated from DP_n determined by GPC analysis. [e] Including long-chain alkyl and pyrene groups in all-*trans* conformation.

Table 2. Diffraction angle and *d* spacings of cellulose and self-assembled cellulose-pyrene nanoparticles.

Samples	$(1\bar{1}0)$		(110)		(200)	
	2θ[a]	d[b]	2θ[a]	d[b]	2θ[a]	d[b]
CELL13	-	-	20.0	0.444	22.1	0.403
CELL13Py	12.2	0.724	19.9	0.447	21.9	0.406
CELL13C15Py	-	-	19.7	0.450	21.8	0.408
CELL30	-	-	-	-	-	-
CELL30Py	-	-	20.0	0.444	21.9	0.404
CELL30C15Py	-	-	19.8	0.448	21.8	0.407
Cellulose I	14.8	0.600	16.2	0.547	22.5	0.394
Cellulose II	12.0	0.739	19.7	0.451	21.8	0.407

[a] Diffraction angle (°). [b] *d* spacing (nm)